

Enhanced VOCs gas mixture recognition with sensor array and SSA-BP neural network

Dang Thi Thu Ha^{1, 2, 3*}, Nguyen Dinh Van², Nguyen Van Duy³, Nguyen Duc Hoa³

¹Hoalu University, 385 Xuan Thanh, Hoa Lu, Ninh Binh, Vietnam;

²School of Electrical and Electronic Engineering, Hanoi University of Science and Technology, 1 Dai Co Viet, Bach Mai, Hanoi, Vietnam;

³School of Materials Science and Engineering, Hanoi University of Science and Technology, 1 Dai Co Viet, Bach Mai, Hanoi, Vietnam.

*Corresponding author: dttha.nth@hluv.edu.vn

Received 4 Sep. 2025; Revised 5 Nov. 2025; Accepted 10 Dec. 2025; Published 25 Dec. 2025.

DOI: <https://doi.org/10.54939/1859-1043.j.mst.108.2025.105-112>

ABSTRACT

Accurate identification of VOCs in mixtures is essential for monitoring toxic and explosive gases, serving industrial, environmental, as well as military and defense applications. In this study, a Salp Swarm Algorithm-Back Propagation (SSA-BP) neural network was proposed in combination with a MEMS-based nano-SnO₂ sensor array to enhance mixed-gas detection. The nano SnO₂ sensors offer high sensitivity, while the SSA-BP neural network optimizes data processing based on noise filtering, feature extraction, and a robust nonlinear learning model, thus improving recognition accuracy, thereby improving recognition accuracy. This combination achieved excellent classification results for mixed gases, with a classification accuracy of up to 99% for various indoor toxic gas mixtures, including acetone, ethanol, and methanol. Additionally, it attained an R-squared score of 0.95 for accurately predicting gas concentrations. Based on the experimental results, we also propose reducing the number of sensors required while maintaining system performance. This integration shows great potential for real-time gas monitoring, as well as for portable VOCs detection systems and safety applications.

Keywords: Gas recognition; Mixed gases; Sensor array; Neural network.

1. INTRODUCTION

A mixture of ethanol, acetone, and methanol poses significant health risks to humans in both industrial and environmental settings [1]. Ethanol may induce respiratory irritation and intoxication at high concentrations, acetone can cause respiratory and neurological effects upon overexposure, and methanol is particularly toxic, leading to blindness or death if ingested [2]. Gas concentrations exceeding safety thresholds can easily cause fires or explosions. The precise detection and recognition of mixed gases, including air quality monitoring, industrial safety, and process control, play a pivotal role in various industrial, environmental, and military domains.

Metal oxide semiconductors (MOS), particularly tin dioxide (SnO₂), have emerged as the leading choice for gas sensing applications owing to their high sensitivity, rapid response time, and cost-effectiveness [3]. Advancements in nanotechnology have further enhanced the performance of SnO₂ sensors by providing a larger surface area for gas interactions, thereby improving their detection capabilities at lower concentrations [4]. Despite these advancements, the challenge remains in the accurate discrimination of mixed gases, where multiple gases are simultaneously present. Traditional signal processing and pattern recognition techniques often struggle to effectively analyze the complex responses generated by mixed gases, leading to inaccurate or unreliable detection [5].

In response to this challenge, machine learning approaches, including various algorithms, have been explored for their ability to model complex nonlinear relationships inherent in sensor data [6]. Although the overall performance improved, the results remained below expectations. Wen et

al. (2019) introduced a 1D-DCNN to automatically extract features and identify components in ethylene–CO–methane mixtures. Compared with SVM, ANN, KNN, and RF, the model achieved superior accuracy (96.30%) under ten-fold cross-validation [7]. Pareek et al. proposed an adaptive ensemble network for gas identification based on a two-dimensional convolutional neural network (2D-CNN) in 2021. The accuracy of the model for gas mixture classification was 91% [8]. In 2022, Wang et al. proposed a multitask convolutional neural network with a dual-block knowledge-sharing structure designed to train a model for the E-nose system. The accuracy of the three tasks for the 12 types of VOCs was approximately 95% when only 4 s of sensing data were used during the response status of the E-nose [9].

The Back Propagation neural network (BPNN) is a widely used method owing to its robustness in training and its ability to generalize data. However, BPNNs are susceptible to local minima, which can impede their performance in certain scenarios. To overcome the limitations of BPNNs, we propose an innovative approach that integrates the Salp Swarm Algorithm (SSA) with the BPNN. By leveraging the SSA's capability to explore the global search space and the BPNN's strength in local optimization, the combined SSA-BP neural network aims to enhance the accuracy and reliability of mixed gas recognition.

This paper presents the design and implementation of a gas sensor array using nano SnO₂ and MEMS (Micro-Electro-Mechanical Systems) coupled with an SSA-BP neural network for improved mixed-gas detection. Our experimental results showed an optimal performance for both classification and concentration prediction. Additionally, we explored the potential for reducing the number of sensors required while maintaining high detection performance, thereby offering a cost-effective and efficient solution for real-time gas monitoring

2. EXPERIMENTS AND DATASET

2.1. Sensor array design

The array composed of ten sensors was fabricated on a glass substrate without backside etching to reduce heat loss using MEMS technology. The sensor array consists of five SnO₂ thin-film sensors sensitized with Pt (CH1–CH5) and five SnO₂ thin-film sensors sensitized with Ag (CH6–CH10), all operating at 200, 250, 300, 350, and 400 °C, as illustrated in figure 1. The sensor array was tested for various VOCs gases. The details and characteristics of the sensor array can be found in [10].

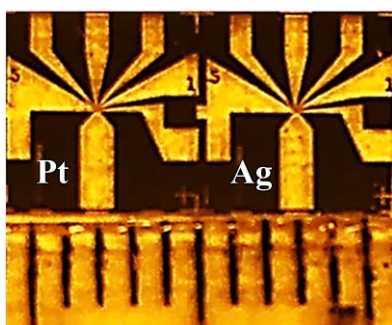


Figure 1. Photograph of the sensor array.

2.2. Mixed gas data collection method

Three VOC gases were measured at nine concentration points based on the safety threshold limits calculated in milliliters according to the static measurement method. The concentrations of ethanol, acetone, and methanol were 0 - 2500, 0 - 4000, and 0 - 2200 ppm, respectively. Three gases were mixed: ethanol, acetone, and methanol. The resulting mixture was divided into eight classes corresponding to the presence of gases. The concentrations of the three gases were

measured at nine distinct points in accordance with the safety assurance thresholds, and the corresponding results are presented in table 1.

Table 1. Mixture of ethanol, acetone, and methanol.

Mix VOCs	Ethanol	Acetone	Methanol	Class	Num	Times
No Gas	0	0	0	1	1	4
Ethanol	1	0	0	2	9	4
Acetone	0	1	0	3	9	4
Methanol	0	0	1	4	9	4
Ethanol Acetone	1	1	0	5	9	4
Ethanol Methanol	1	0	1	6	9	4
Acetone Methanol	0	1	1	7	8	4
Ethanol Acetone Methanol	1	1	1	8	81	4
Sum					135	

2.3. Experiment for measuring VOC gas mixtures and dataset

A schematic of the gas mixing and measurement system is shown in figure 2. The standard gases were mixed to achieve the required dilution concentrations of Ethanol, Acetone, and Methanol. The gas mixture was then injected into the measurement chamber. The sensor array system, consisting of a surface-modified Pt/Ag Nano SnO₂ thin film integrated with ten sensors, was placed in the measurement chamber to respond to the gas mixture. The data acquisition system for the sensor array was connected to a computer via a USB and controlled using an application program written in the LabVIEW programming language.

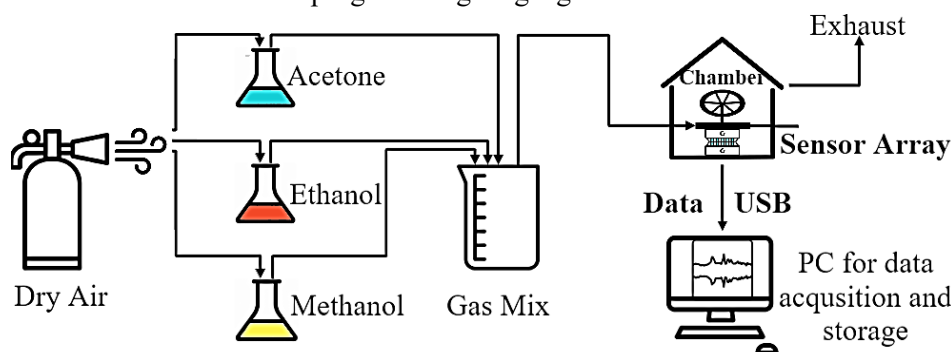


Figure 2. Schematic diagram of the gas mixture measurement system.

The dataset consisted of 135 different concentration mixtures of three VOC gases: Ethanol, Acetone, and Methanol, and each mixture concentration was measured four times. The dataset included 43,200 rows and 18 columns. The data from the 10 sensors were labeled with concentrations of Ethanol, Acetone, and Methanol in various gas mixtures and classified into eight distinct data categories.

3. ALGORITHM AND NETWORK STRUCTURE

3.1. The SSA-BP algorithm

SSA is a nature-inspired optimization algorithm that can effectively explore the search space and avoid local minima, thereby providing a more global optimization of weights and biases [11, 12].

By finding a better set of initial weights and biases, SSA can improve the accuracy of the neural network. The subsequent fine-tuning with backpropagation starts from a better position, leading to better overall performance. Figure 3 illustrates the representation diagram of the algorithm.

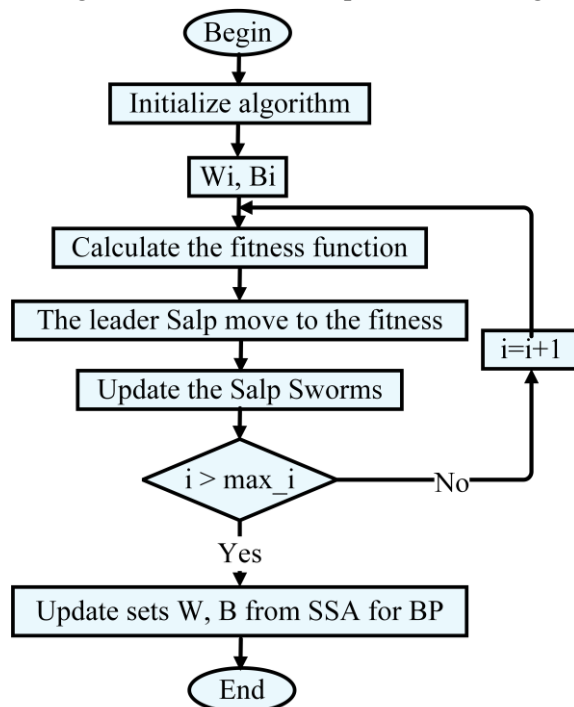


Figure 3. SSA-BP algorithm.

The steps for implementing a BP Neural Network are as follows:

1. Select the best solution from the SSA. After the SSA converges or reaches the maximum number of iterations, the best solution (weights and biases) is selected from the SSA process as the initial weights for the neural network.
2. Forward propagation: Calculate the output of each layer based on the input of that layer and the current weights and biases. An activation function was used to compute the output of each neuron.
3. Backward propagation: Compute the gradient of the error function with respect to each weight and bias using the chain rule. This gradient indicates the extent to which each weight and bias must be adjusted to reduce errors.
4. Update weights and biases: Update weights using the Adam algorithm and adjust the weights and biases based on the gradient and learning rate.
5. Repeat steps 2 - 5 until the error reaches an acceptable level or after a set number of iterations.

3.2. Network structure

The network structure of the SSA-BP model used in this process is shown in figure 4, and includes an input layer, three hidden layers, and an output layer.

The input contained ten features that were fed into the first hidden layer. The first hidden layer contained 32 neurons and the ReLU activation function was used to calculate the neurons. The output of the first hidden layer served as the input to the second hidden layer, which also contained 32 neurons and used the ReLU activation function. The output of the third hidden layer was then fed into the output layer, which contained eight neurons. These neurons use the Softmax activation function to convert their values into probabilities suitable for multiclass classification. The network performance was optimized using the MAE loss function and Adam optimizer.

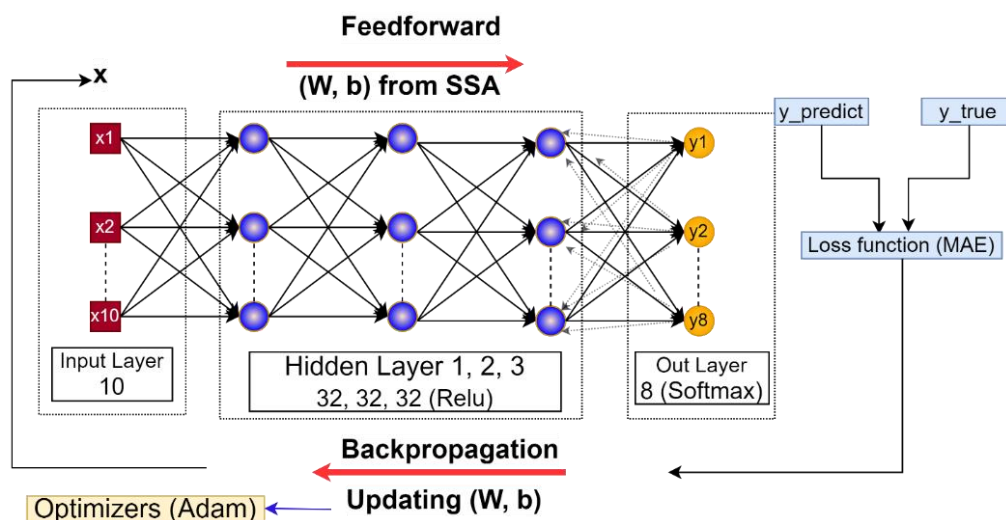


Figure 4. Structure of SSA-BP neural network.

4. RESULTS AND DISCUSSION

4.1. Comparison of machine learning models

In this study, 20% of the data were used for testing, and the remaining 80% were used for training. Five-fold cross-validation was used throughout all processes to adjust the model parameters and evaluate the final model performance. The initial learning rate of all SSA-BPNN models was 0.001, and the batch size was 5.

The performance of six machine learning models, SSA-BP, BP, SVC, RF, MLP, and KNN, was evaluated based on F1-scores across eight classes and overall accuracy. The F1-score combines precision and recall, making it particularly useful for imbalanced datasets. As shown in table 2, SSA-BP demonstrated the highest performance with F1-scores consistently close to 1.0 across all classes and the highest overall accuracy of 0.99. This indicates superior generalization capabilities and precise predictions. MLP (Multi-Layer Perceptron) exhibits lower performance, particularly in classes 4, 5, and 7, and has a lower overall accuracy of 0.95. Finally, KNN performed the worst, with the lowest F1-scores across most classes and the lowest accuracy of 0.90, indicating its limitations for this dataset.

Table 2. Performance evaluation of machine learning models in classification.

CLASS	F1-score					
	SSA-BP	BP	SVC	RF	MLP	KNN
1	1	1	1	1	1	1
2	0.99	0.97	0.97	0.97	0.95	0.90
3	0.99	0.97	0.96	0.97	0.97	0.93
4	0.99	0.95	0.95	0.96	0.89	0.82
5	0.98	0.96	0.96	0.95	0.88	0.75
6	0.98	0.94	0.94	0.93	0.89	0.78
7	0.97	0.97	0.92	0.94	0.84	0.80
8	1	0.98	0.97	0.96	0.96	0.94
Accuracy	0.99	0.97	0.95	0.94	0.93	0.90

The differences in the F1-scores among the models primarily resulted from their distinct learning and optimization capabilities. The SSA effectively optimizes the initial weights of the BP

network, avoiding local minima and better capturing nonlinear and overlapping gas patterns. The BP, SVC, and RF models showed relatively good performance, but were less stable in classes with overlapping feature distributions. The MLP and KNN models yield lower F1-scores owing to their sensitivity to noise and inefficiency in high-dimensional feature spaces.

Table 3 provides a comparative evaluation of the metrics of the five mixed-gas concentration regression algorithms. The SSA-BP Regression achieved the highest R-squared value of 0.95, showing the best modeling and prediction ability. Both MSE (0.04) and MAE (0.08) were the lowest, demonstrating the ability to maintain small, squared errors and standard deviations, thus helping the model to have high prediction stability.

Table 3. Performance evaluation of machine learning models in predicting concentration.

Algorithm name	R-square	MSE	MAE
SSA-BP regression	0.95	0.04	0.08
Support vector regression	0.94	0.05	0.11
K-Nearest Neighbors regression	0.93	0.07	0.09
Extreme Gradient Boosting regression	0.91	0.19	0.10
Linear Regression	0.61	0.51	0.38

KNN stands out for its low absolute error (MAE), while Extreme Gradient Boosting is also an effective solution, particularly when optimizing problems with complex data. Linear Regression, on the other hand, does not respond well to the requirements of predicting gas mixture concentrations, due to its low performance and high error. The results indicated that the SSA-BP model achieved the highest performance for both gas classification and concentration prediction.

4.2. Sensor array optimization

This study reduced the number of active sensors used to investigate array optimization. Accordingly, the dimensions of the input data array change from 10 to 1, depending on the specific study requirements. When a particular array width is required, the data from the remaining sensors is discarded. Because no significant difference between the roles of the various sensors was detected, the sensors were excluded in a random order. This allowed us to establish a relationship between the model performance and the number of active sensors.

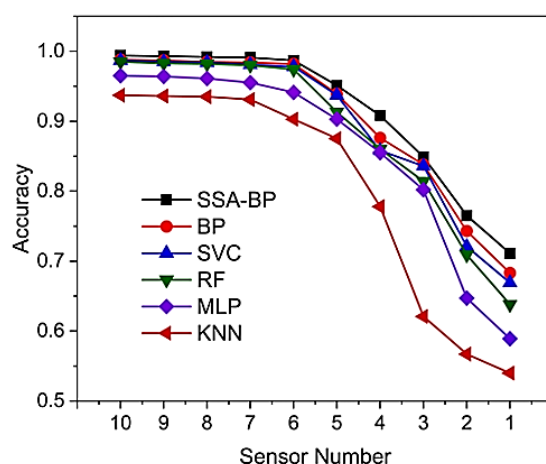


Figure 5. Array optimization results of classification models.

The results of the classification models were evaluated, as shown in figure 5. All models displayed a common trend: the performance declined as the number of active sensors decreased. The slope of

the decline encountered a turning point under the 4-sensor condition. Before the number of active sensors was reduced to four, the performance of most models showed a slow linear decline, except for KNN. The performance of the models was not significantly influenced by changes in the number of active sensors. SSA-BP remained the leading model, followed by BP, SVC, RF, MLP, and KNN. It maintained the highest accuracy across all sensor counts, ranging from 0.99 with 10 sensors to 0.71 with one sensor. On average, the SSA-BP model achieved 99% accuracy when the number of sensors was reduced by four. Reducing the number of sensors in a multisensor system not only offers cost and performance benefits but also enhances the reliability, security, and maintainability of the system. This is particularly crucial in industrial and environmental applications, where high efficiency and durability of the monitoring system are required.

5. CONCLUSIONS

In this study, we developed an innovative approach for the recognition of mixed gases using a nano SnO₂ sensor array coupled with an SSA-BP neural network. The combination of the high sensitivity of the nano SnO₂ sensors and the powerful optimization capabilities of the SSA-BP neural network resulted in a significant enhancement in the accuracy of mixed-gas detection. Our experimental results demonstrated a classification accuracy of up to 99% for mixtures of VOC gases. In addition, the average success rate for predicting concentration levels during the testing phase was 0.95%. Moreover, we propose an optimization strategy to reduce the number of sensors required without compromising the performance of the system, thereby enhancing the cost-effectiveness, energy efficiency, and practicality of the solution. However, the study was limited by the specific types of gas mixtures tested and controlled experimental conditions. To validate its effectiveness, future studies should explore the applicability of this method to a wider range of gases and real-world environmental conditions to validate its effectiveness.

REFERENCES

- [1]. P. Wei, L. Luling, L. Peitao, “*Detection and treatment of VOC in the food industry*”, International Journal of Agriculture and Food Sciences Research, Vol. 1, pp. 115–123, (2024).
- [2]. L. Kyle, N. Kumar, “*Pulmonary health effects of indoor volatile organic compounds: A meta-analysis*”, International Journal of Environmental Research and Public Health, Vol. 18, p. 1578, (2021).
- [3]. H. Nazemi, A. Joseph, J. Park, A. Emadi, “*Advanced micro- and nano-gas sensor technology: A review*”, Sensors (Switzerland), Vol. 19, No. 6, (2019).
- [4]. G. F. Fine, L. M. Cavanagh, A. Afonja, R. Binions, “*Metal oxide semiconductor gas sensors in environmental monitoring*”, Sensors, Vol. 10, pp. 5469–5502, (2010).
- [5]. N. Barsan, D. Koziej, U. Weimar, “*Metal oxide-based gas sensor research: How to?*”, Sensors and Actuators B: Chemical, Vol. 121, pp. 18–35, (2007).
- [6]. P. Pławiak et al., “*A new deep genetic hierarchical network of learners for prediction of credit scoring*”, Information Sciences, Vol. 516, pp. 401–418, (2020).
- [7]. X. Zhao, Z. Wen, X. Pan, W. Ye, A. Bermak, “*Mixture gases classification based on multi-label one-dimensional deep convolutional neural network*”, IEEE Access, Vol. 7, pp. 12630–12637, (2019).
- [8]. V. Pareek, S. Chaudhury, S. Singh, “*Online pattern recognition of time-series gas sensor data with adaptive 2D-CNN ensemble*”, Proceedings of IDAACS, Vol. 2, pp. 679–683, (2021).
- [9]. T. Wang et al., “*Target discrimination, concentration prediction, and status judgment of electronic nose system based on large-scale measurement and multi-task deep learning*”, Sensors and Actuators B: Chemical, Vol. 351, (2022).
- [10]. N. Van Duy et al., “*Design and fabrication of effective gradient temperature sensor array based on bilayer SnO₂/Pt for gas classification*”, Sensors and Actuators B: Chemical, Vol. 351, p. 130979, (2022).
- [11]. S. Mirjalili, A. H. Gandomi, S. Z. Mirjalili, S. Saremi, H. Faris, S. M. Mirjalili, “*Salp swarm algorithm: A bio-inspired optimizer for engineering design problems*”, Advances in Engineering Software, Vol. 114, p. 163, (2017).
- [12]. B. Zhang, X. Tao, H. Zhang, J. Yu, “*Study of an SSA-BP neural network-based strength prediction model for slag-cement-stabilized soil*”, Materials, Vol. 18, No. 15, p. 3520, (2025).

TÓM TẮT

Tăng cường nhận dạng hỗn hợp khí VOCs bằng mảng cảm biến và mạng nơ-ron SSA-BP

Việc nhận dạng chính xác các khí VOCs trong hỗn hợp là hết sức cần thiết nhằm giám sát các loại khí độc hại và dễ cháy nổ, phục vụ cho các ứng dụng trong công nghiệp, môi trường, cũng như trong quân sự và quốc phòng. Nghiên cứu này đề xuất mạng nơ-ron SSA-BP kết hợp với mảng cảm biến nano-SnO₂ dựa trên công nghệ MEMS nhằm nâng cao hiệu quả phát hiện khí. Các cảm biến nano-SnO₂ mang lại độ nhạy cao, trong khi mạng SSA-BP tối ưu hóa quá trình xử lý dữ liệu nhờ lọc nhiễu, trích rút đặc trưng và mô hình học mạnh mẽ với dữ liệu phi tuyến. Hệ thống đạt độ chính xác phân loại tới 99% với các hỗn hợp acetone, ethanol và methanol, cùng hệ số R² là 0,95 trong dự đoán nồng độ. Ngoài ra, số lượng cảm biến có thể được tối giản mà vẫn duy trì hiệu năng. Sự tích hợp này cho thấy tiềm năng lớn trong các ứng dụng giám sát khí theo thời gian thực, phát hiện VOCs trên thiết bị di động và các ứng dụng an toàn.

Từ khoá: Nhận dạng khí; Hỗn hợp khí; Mảng cảm biến; Mạng nơ-ron.